Journal of Medicinal Chemistry

Article

pubs.acs.org/jmc

"True" Antiandrogens—Selective Non-Ligand-Binding Pocket Disruptors of Androgen Receptor–Coactivator Interactions: Novel Tools for Prostate Cancer

Laura Caboni,[†] Gemma K. Kinsella,[†,∥] Fernando Blanco,[†] Darren Fayne,[†] William N. Jagoe,[†] Miriam Carr,[†] D. Clive Williams,[‡] Mary J. Meegan,[§] and David G. Lloyd*[,†]

[†]Molecular Design Group, School of Biochemistry and Immunology, [‡]School of Biochemistry and Immunology, and [§]School of Pharmacy and Pharmaceutical Sciences, Trinity Biomedical Sciences Institute, Trinity College Dublin, Dublin 2, Ireland

Supporting Information

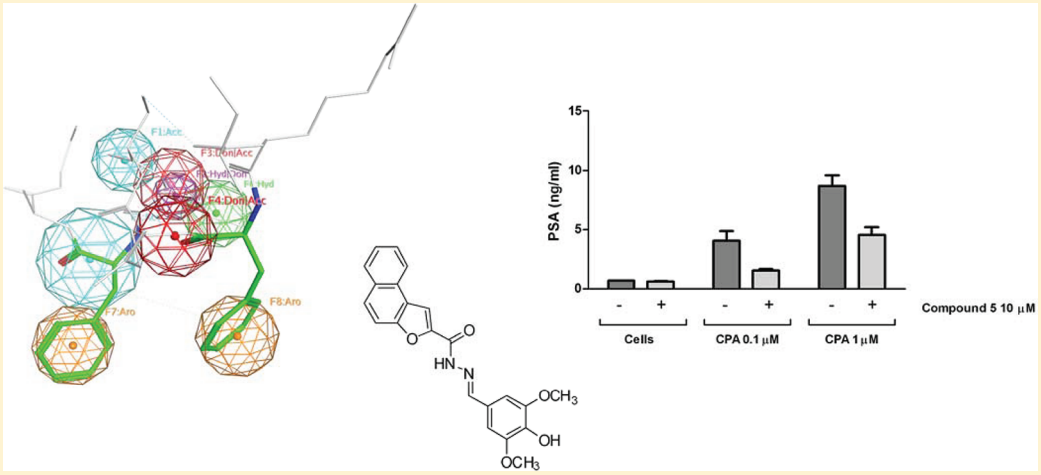

ABSTRACT: Prostate cancer (PCa) therapy typically involves administration of "classical" antiandrogens, competitive inhibitors of androgen receptor (AR) ligands, dihydrotestosterone (DHT) and testosterone (tes), for the ligand-binding pocket (LBP) in the ligand-binding domain (LBD) of AR. Prolonged LBP-targeting leads to resistance, and alternative therapies are urgently required. We report the identification and characterization of a novel series of diarylhydrazides as selective disruptors of AR interaction with coactivators through application of structure and ligand-based virtual screening. Compounds demonstrate full ("true") antagonism in AR with low micromolar potency, selectivity over estrogen receptors α and β and glucocorticoid receptor, and partial antagonism of the progesterone receptor. MDG506 (**5**) demonstrates low cellular toxicity in PCa models and dose responsive reduction of classical antiandrogen-induced prostate specific antigen expression. These data provide compelling evidence for such non-LBP intervention as an alternative approach or in combination with classical PCa therapy.

INTRODUCTION

Prostate cancer (PCa) is one of the major causes of cancer death in men worldwide.[1] The molecular basis of the disease involves an irregular behavior of the functions mediated by the androgen receptor (AR). Human AR belongs to the nuclear receptor (NR) superfamily of transcription factors, which regulate gene transcription upon ligand binding.[2] The structure of NRs is extensively documented in the literature,[3] and in general, NRs share the following common organization: a variable amino-terminal activation function domain (AF-1), a highly conserved DNA-binding domain (DBD), a hinge region that contains the nuclear localization signal, a conserved C-terminal ligand-binding domain (LBD) comprising a 12 helical structure that encloses a central ligand binding pocket (LBP), and a second activation function domain (AF-2) that is located at the carboxy-terminal end of the LBD and mediates ligand-dependent transactivation.

AR is activated by the endogenous hormone testosterone (tes) and its more potent metabolite dihydrotestosterone (DHT), both of which bind in the LBP. The binding of these endogenous modulators induces a reorganization of helix 12 to the so-called "agonist" conformation, generating a structured hydrophobic surface (AF-2) suitable for the recruitment of tissue-specific NR coactivators. Such NR coactivators can be thought of as "master switches", directing and amplifying the subsequent transcriptional activity of the target NR. In a recent work, an additional secondary function site called binding function 3 (BF-3) has been reported on the surface of the AR

Received: October 25, 2011
Published: January 26, 2012

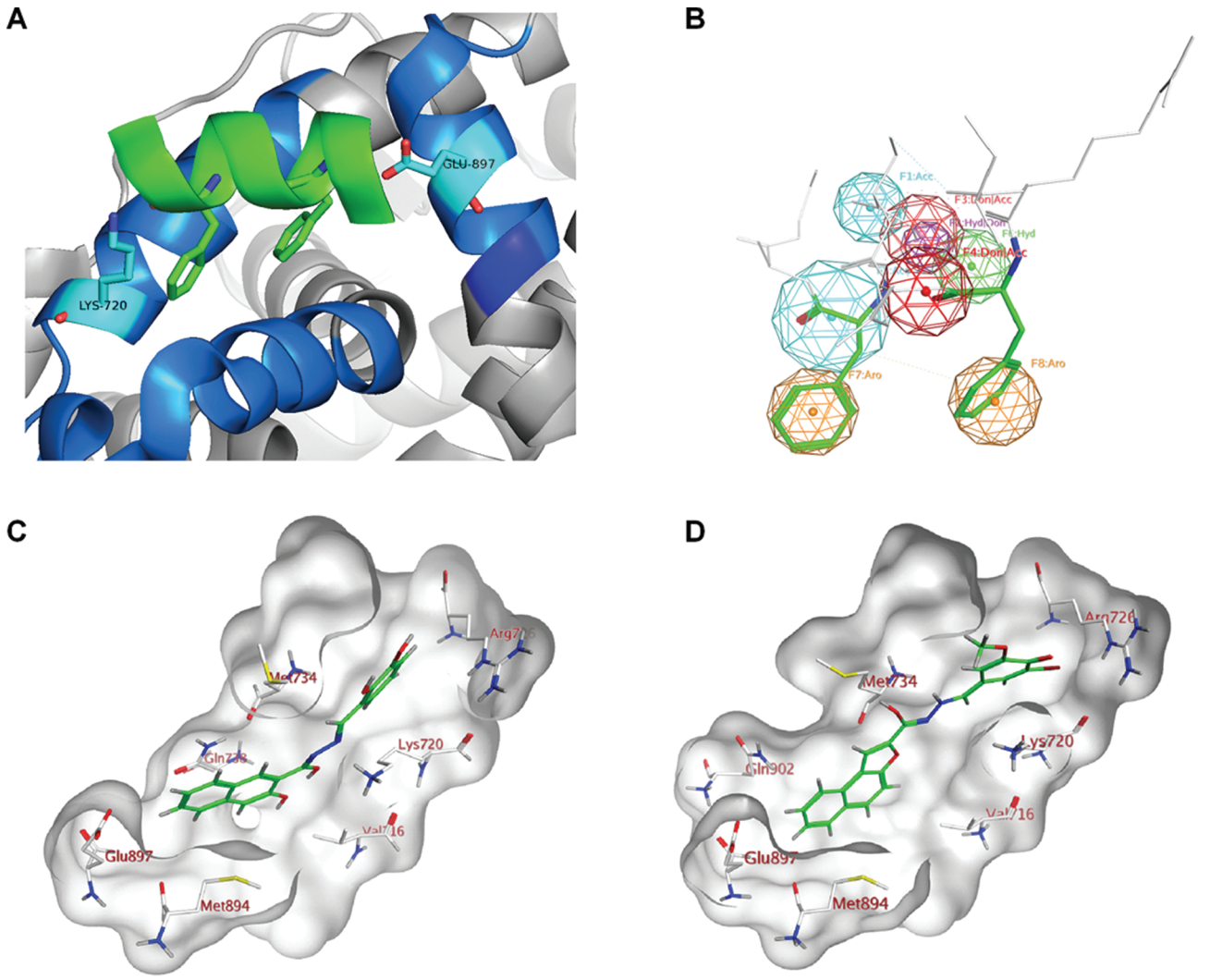

Figure 1. Virtual screening and identification of diarylhydrazide scaffolds. (A) A series of coactivator peptides cocrystallized in the AF-2 groove was employed; for illustrative purposes we present the FxxLF coactivator motif from PDB entry 1T7R. The AF-2 groove is represented in dark gray. For clarity reasons, only Lys720 and Glu897 are shown and DHT is not illustrated;[23] (B) A 3D pharmacophore model was derived containing the common features between AR coactivators and the two aromatic features of the FxxLF motif. Pharmacophores were used to screen vendor compound databases and to guide the docking of putative "hits" into the AF-2 site. The screen identified an active diarylhydrazide class of compounds. (C, D) Two first round actives **1** (MDG173) and **2** (MDG15) docked poses in the AF-2 site, with the surface rendered and only key amino acids shown. Partial mapping of initial hits to the pharmacophore suggested additional virtual screening to identify more potent family members. Images were generated with Molecular Operating Environment (MOE)[25] and PyMol.[26]

that could also play a relevant role in the allosteric modulation of the AF-2.[4]

NR drug development has traditionally focused on advancing full or partial agonists/antagonists interacting within the LBP of the LBD.[5] PCa has been treated by intervention at the early stages through utility of classical antiandrogens, which act by displacing the natural hormones from the pocket and inducing a conformational change of the helix 12 so that coactivators cannot be recruited. Tissue specificity, detrimental side effects, and a loss of the pharmacological effect (acquired drug resistance) over time are major and ongoing concerns with such LBP targeting treatment regimes.[6,7]

It has been demonstrated that it is possible to inhibit the transcriptional activity of the NRs by directly blocking the critical receptor:coactivator interaction.[8−13] This alternative approach to traditional NR modulation may furnish greater pharmacological insight and afford opportunities to modulate not only under tissue specific circumstances but without adversely affecting natural ligand binding and so preserving the beneficial/nondisease linked functions of the receptors. Specifically, the steroid receptor coactivator (SRC) family has been postulated as a feasible target for pharmacological intervention.[14] The viability of targeting AR−coactivator interaction using small molecules has been recently demonstrated.[4,8] Moreover, it has been postulated that circumventing the LBP will overcome the problem of drug resistance in PCa.[15−19]

Here we describe the discovery and characterization of a novel class of selective non-LBP "true" antiandrogens, characterized by full AR antagonism in inhibiting the recruitment of coactivators and lacking intrinsic partial agonistic properties. Mechanistically, these compounds are totally differentiated from the recent description of true LBP antiandrogens like MDV3100 and RD162,[20,21] while their selectivity and druglike nature underpin the potential of a non-LBP intervention strategy in advanced prostate cancer resistant

dx.doi.org/10.1021/jm201438f | J. Med. Chem. 2012, 55, 1635−1644

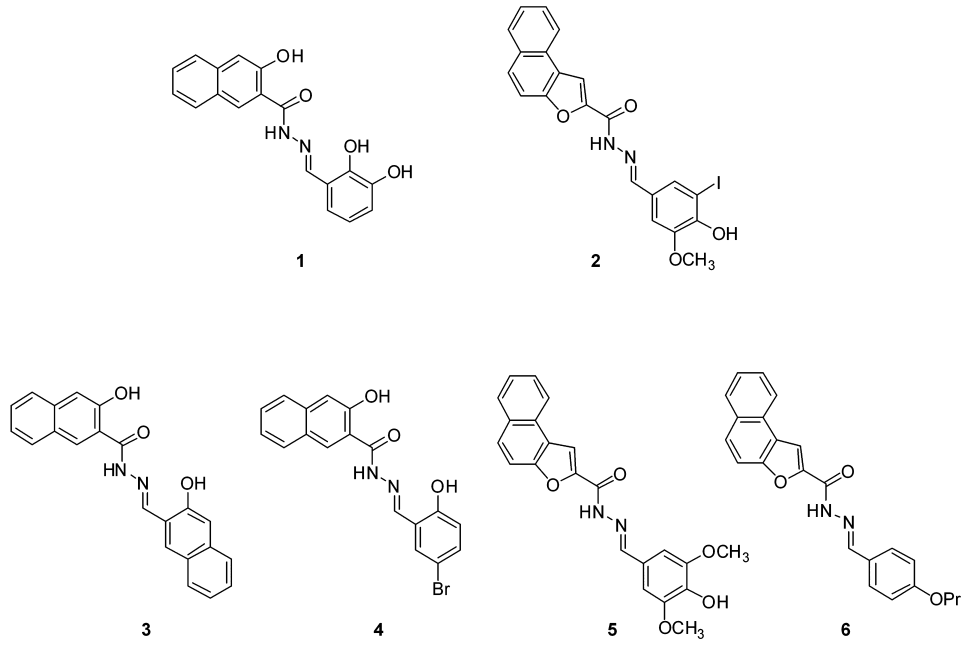

Figure 2. Diaryl-substituted hydrazides retrieved from the virtual screening process.

to "classical therapy", first described for the true non-LBP targeting antiandrogens pyrvinium pamoate (PP) and harmol hydrochloride (HH).[22]

The biological data obtained both on target with time-resolved fluorescence resonance energy transfer (TR-FRET)/fluorescence polarization (FP) assays and in cellular PCa models demonstrate the non-LBP antagonist activity of the series and an alternative mechanism of inhibition, furnishing a new class of nonpeptidic, small molecule AR:coactivator selective disruptors as leads for the development of novel treatments for prostate cancer.

RESULTS

Virtual Screening. A virtual (computational) screen of six vendor compound databases (see Experimental Section) was performed through a combination of 3D pharmacophore generation and docking. Seven X-ray structures of coactivator peptide bound AR were used to define key ligand-derived pharmacophoric features of the most represented motifs occurring in known AR coactivators.[23] Initially, common key interaction motifs within the peptide of the form FxxLF, LxxLL, or FxxLW were considered to generate a consensus AF-2 pharmacophore. Subsequently, a second site-derived pharmacophore model was advanced based on the specific characteristics of the androgen receptor AF-2 region, which demonstrates known selectivity toward the FxxLF coactivator motif[24] (Figure 1B). The cocrystallization of the AR LBD bound with DHT in the presence of the FxxLF peptide (PDB ID 1T7R)[23] provided the structural basis of the AF-2 interaction for docking studies.

From the virtual screen, a first series of compounds with predicted target affinity was selected from commercially available databases (see Experimental Section) and evaluated for biological activity using TR-FRET and FP techniques. This initial screen (Figures 1C,D and 2) identified two small molecules, **1** and **2**, both diarylhydrazides, as possible non-LBP AR antagonists. Non-LBP modulatory activity was evidenced by demonstration of an IC_{50} in the range of 50−100 μM in AR TR-FRET coactivator displacement assay and their inability to displace bound fluorescently labeled ligand from the LBP through an FP assay. These first round "hit" molecules map only partially to the screening pharmacophore (Figure 1C,D). Accordingly, an optimization round of screening was initiated to explore the utility of the scaffold for more effective disruption of AR:coactivator interaction.

From these initial data, a simple molecular similarity search was performed (Tanimoto coefficient >70%) to furnish a new screening series of 37 compounds bearing the desired diarylhydrazide scaffold. This second round screen identified four small molecules (Figure 2), **3** (MDG 483), **4** (MDG 292), **5** (MDG 506), and **6** (MDG 508), with improved activity (IC_{50} < 50 μM in an AR TR-FRET assay). These ligands were taken forward for additional investigation and characterization.

Diarylhydrazides Inhibit FxxLF Coactivator Recruitment by AR without Traditional Antagonism of the LBP. The series of diaryl-substituted hydrazides identified through the VS process (Figure 2) inhibited the recruitment of the fluorescent labeled D11-FxxLF coactivator peptide in the presence of an agonist (DHT) concentration equal to EC_{80} using time-resolved FRET assays. D11-FxxLF is a peptide developed from random phage display technology that resembles the SRC family of coactivator proteins in its flanking sequence but that also has an AR N-terminal interaction domain.[24] Thus, it is a biological mimic of the N-terminal and the SRC coactivator interactions with the LBD.

A 12-point dose−response curve was determined for those compounds that inhibited coactivator binding in the micromolar range, acting as full AR antagonists, **3**−**6** (Figure 3A and Table 1).

Maximal activity was calculated as per established methods.[27] The background signal, representing diffusion-enhanced FRET in the absence of AR, was subtracted from the FRET value of

dx.doi.org/10.1021/jm201438f | J. Med. Chem. 2012, 55, 1635−1644

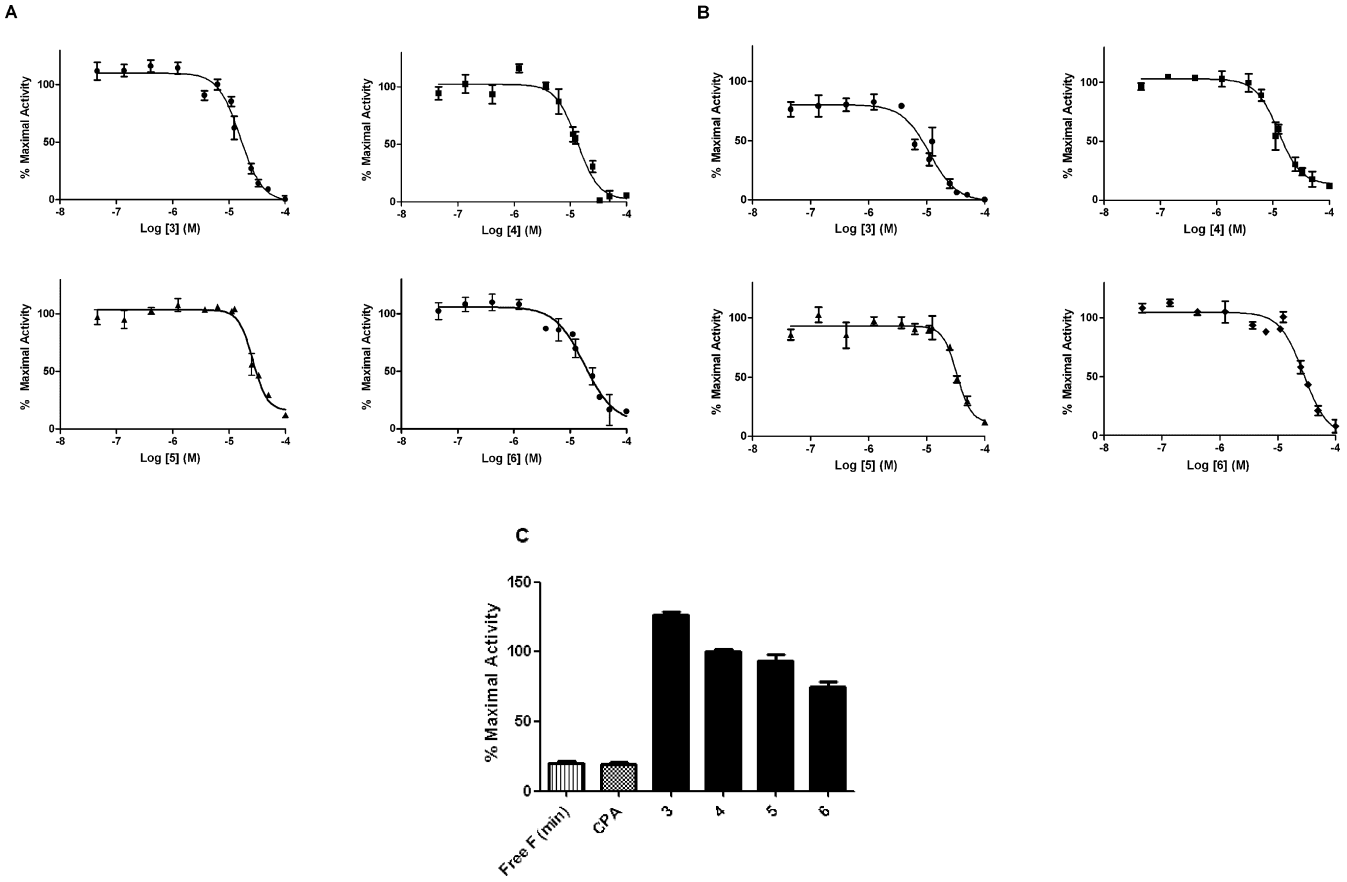

Figure 3. Diarylhydrazides inhibit the AR recruitment of a fluorescent-labeled D11-FxxLF peptide but do not displace a potent fluorescent ligand from the AR-LBP. (A and B) Compounds were tested in a TR-FRET assay across a concentration range from 100 μM to 45 nM in the presence of a concentration of DHT = EC_{80} in AR-LBD wt (A) and AR-LBD T877A (B). Data points represent the mean of two independent experiments performed in triplicate. Error bars represent the standard error of the mean (SEM) for n = 6 values. Data was fitted using log antagonist concentration vs response (variable slope) with GraphPad Prism 5 (see Experimental Section for details). (C) Fluorescence polarization data is plotted as percent maximal activity represented by AR-LBD and fluorophore complex (0% inhibition). The minimum control value represents free fluorophore (Free F) in solution (100% inhibition). Error bars represent the SEM for n = 6 values.

Table 1. Diarylhydrazides Activity toward AR and ART877A[a]

compounds	AR (wt)	AR T877A
3	15.9 ± 3.2 μM	11.1 ± 3.2 μM
4	13.3 ± 3.1 μM	12.4 ± 2.2 μM
5	26.3 ± 3.8 μM	33.2 ± 5.9 μM
6	17.9 ± 6.9 μM	28.1 ± 6.7 μM

[a] IC_{50} values are shown as ±SEM (n = 6). Activity data are in agreement for **4** and **5** in both AR wt and ART877A. The higher confidence mP values and experimental reproducibility obtained for **4** and **5** in coactivator studies were used as the basis to advance these compounds to cellular characterization and receptor subtype selectivity evaluations.

each compound and from the maximal signal, representing FxxLF-bound AR in presence of DHT.

$$(\text{FRET signal} - \text{background})_{\text{compound}} / (\text{FRET max signal} - \text{background})_{\text{DMSO}} \times 100$$

The TR-FRET assay cannot differentiate between direct coactivator antagonists acting on the LBD surface and classical AR antagonists, which also functionally disrupt coactivator recruitment by displacing DHT from the ligand binding pocket. To characterize the nature of the antagonist effect, compounds were tested for their ability to displace a potent fluorescent ligand (fluorophore) from the AR LBP through a fluorescence polarization (FP) assay at a single point concentration (50 μM), using cyproterone acetate (CPA) at the same concentration as a reference, a known AR LBP-mediated antagonist. All compounds tested showed 0% inhibition of the AR-LBD and fluorophore complex, indicating a non-LBP-mediated mechanism of AR transactivation inhibition (Figure 3C).

Compound **3** gave an unusually high value of millipolarization units (mP), 20% higher than the maximal control (Figure 3C). This could be indicative of solubility issues in the assay buffer and therefore could generate a false negative result. It is known that FP assay outcomes can be influenced by intrinsic fluorescence of the test compounds and/or light scattering phenomena due to poor solubility and precipitation. To minimize the possibility of such false negative or positive reporting, the FP data was rigorously interrogated through examination of both autofluorescence and aggregation. None of the compounds tested showed competing autofluorescence in the assay conditions or was shown to be a false negative. Results are shown in the Supporting Information (Supplementary Figure 2).

dx.doi.org/10.1021/jm201438f | J. Med. Chem. 2012, 55, 1635−1644

To further validate the utility of these ligands in PCa, on-target binding experiments were also performed using the recombinant T877A AR mutant[28,29] characteristic of advanced stage androgen-independent PCa. In TR-FRET, the compounds demonstrated similar activity to that observed in the wild type assays, indicating their potential in advanced phases of prostate cancer (Figure 3B).

Diarylhydrazides Are AR Selective Coactivator Interaction Disruptors. We undertook to profile the selectivity of these compounds for AR over other members of the same phylogenetic branch of the steroidal nuclear receptor subfamily. Compound binding affinities for progesterone receptor (PR), glucocorticoid receptor (GR), estrogen receptor α (ER-α), and estrogen receptor β (ER-β) were determined using TR-FRET (Table 2). Diarylhydrazides do not displace fluorescent-labeled coactivator PGC-1α from estradiol−ER-α and estradiol−ER-β complex and do not displace fluorescent-labeled coactivator SRC1-4 from dexamethasone−GR complex at concentrations up to 100 μM (Supporting Information, Supplementary Figures 3−5). Compound **5** binds PR with comparable affinity to that observed for AR, while **4** demonstrates approximately 2-fold binding selectivity for the AR over PR.

Table 2. Diarylhydrazides Activity (IC_{50}, μM) in GR, ER-α/ER-β, and PR Nuclear Receptor Targets[a]

compounds	GR	ER-α	ER-β	PR
4	NA (>100)	NA (>100)	NA (>100)	22.5 ± 5.4
5	NA (>100)	NA (>100)	NA (>100)	27.7 ± 7.3

[a]Data are presented as averages of at least two independent experiments. IC_{50} values are shown as ±SEM (n = 6). NA = not active at 100 μM.

In functional evaluation we determined that the diarylhydrazide compounds are full AR antagonists, with a partial antagonistic profile demonstrated in PR, displacing SRC1−4 from progesterone−PR complex at micromolar concentrations (Figure 4 and Table 2).

The non-LBP nature of this interaction was confirmed by an FP assay (Supporting Information, Supplementary Figure 6).

Diarylhydrazides Demonstrate Low Toxicity in Different Prostate Cancer Cellular Models. To ascertain the translational (clinical) potential of these ligands, compounds were evaluated in cellular models of prostate cancer (LNCaP,[30] an androgen-dependent cell line and PC-3,[31] an androgen-independent cell line) and in normal prostatic epithelia cell line PWR-1E.[32] Cell viability was assessed after 24 h of incubation with the test compounds at three different concentrations (Figure 5). The classical antiandrogen CPA was used as a reference, showing a minor effect at 50 μM in the androgen independent cell line PC-3. At 50 μM **4** reduces cell viability to a 50−60%, whereas **5** acts consistently across the three cell lines, retaining cell viability at around 80%. These data suggested **5** as a potential candidate for further functional characterization.

Compound 5 Reduces DHT-Dependent Cell Proliferation in LNCaP. The diarylhydrazides were evaluated for their effects on the AR signaling pathway and on hormone-dependent cellular growth of LNCaP cells. Compound **5** was well-tolerated after 5 days of treatment at 10 and 20 μM concentrations and enabled observation of a specific reduction in DHT-treated cell count (Figure 6A).

Compound 5 Reduces DHT- and CPA-Stimulated PSA Expression in LNCaP Cells. Prostate specific antigen (PSA) is a serine protease normally secreted by the prostate epithelia. Its expression is under the control of AR. PSA is widely used as a marker for PCa[33], as its serum levels are increased in this condition. Compound **5** was shown to reduce DHT-induced PSA secretion in a dose−response fashion as quantified by an ELISA experiment in LNCaP cells (Figure 6B).

It is well-documented that classical antiandrogens (i.e., those binding within the LBP/competing with endogenous ligands) have partial agonistic properties, which make them less useful in the management of advanced prostate cancer.[34] Arising from this inherent agonism, in an androgen-deprived LNCaP cell line, antiandrogens such as CPA can actually *activate* the AR pathway and stimulate cell growth.[35] In direct contrast to the behavior of traditional antagonists, **5** shows no detectable agonist or partial agonist activity at tested concentrations, consistent with an alternative mechanism to that of the classical antiandrogens. Finally, treatment with **5** at 10 μM was found to antagonize CPA partial agonist activity (measured as secreted PSA levels in the cellular media in an ELISA experiment), suggesting its potential benefit in combination therapy for advanced stages of prostate cancer (Figure 6C). To further challenge this hypothesis, the compounds were characterized in the 22Rv1 cell line.[36] This castration resistant cell line expresses the AR H874Y mutation. The compounds also demonstrated

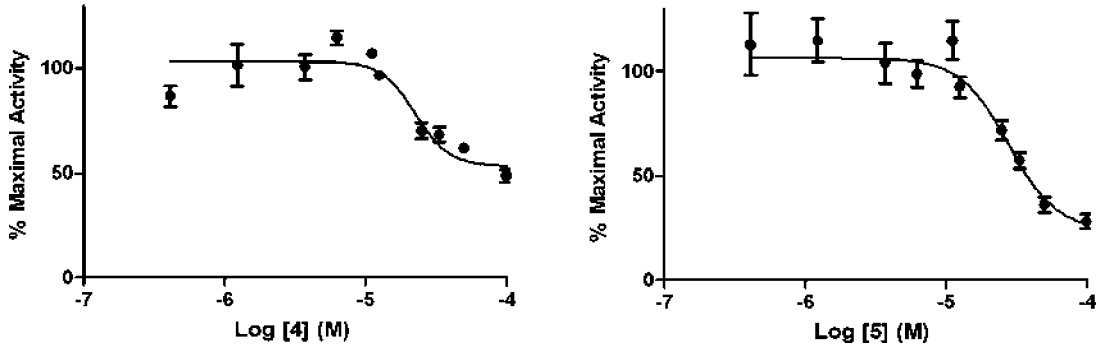

Figure 4. Compounds **4** and **5** are partial antagonists for PR. Compounds were tested at a concentration range from 100 to 1 μM in the presence of a concentration of progesterone = EC_{80}. Data points represent the mean of two independent experiments in triplicate. Error bars represent the standard error of the mean (SEM) for n = 6 values. Data was fitted using log antagonist concentration vs response (variable slope) with GraphPad Prism 5 (see Experimental Section for details). Compounds **4** and **5** show 50% and 30% inhibition respectively at 100 μM. IC_{50} values are shown in Table 2.

dx.doi.org/10.1021/jm201438f | J. Med. Chem. 2012, 55, 1635−1644

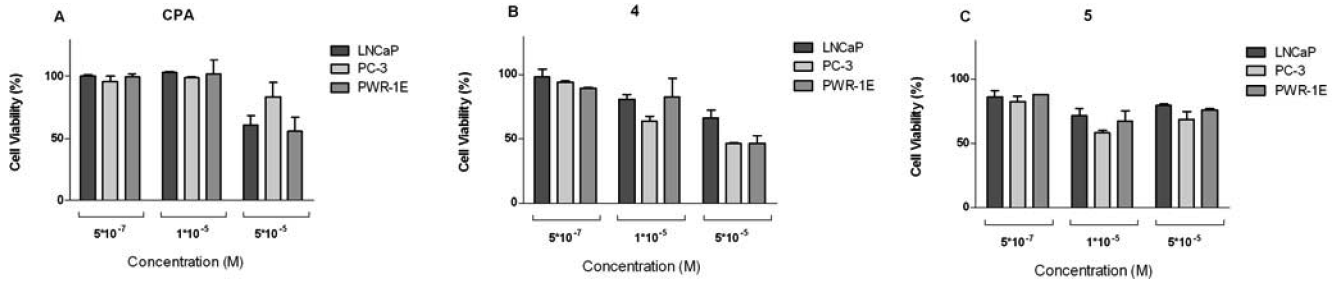

Figure 5. Cell viability profile in LNCaP, PC-3, and PWR-1E cell lines. %Percent cell viability is plotted against the molar compound concentrations. Compounds were tested at 5×10^{-5}, 1×10^{-5}, and 5×10^{-7} M. Error bars represent the SEM of two independent experiments done in triplicate (n = 6).

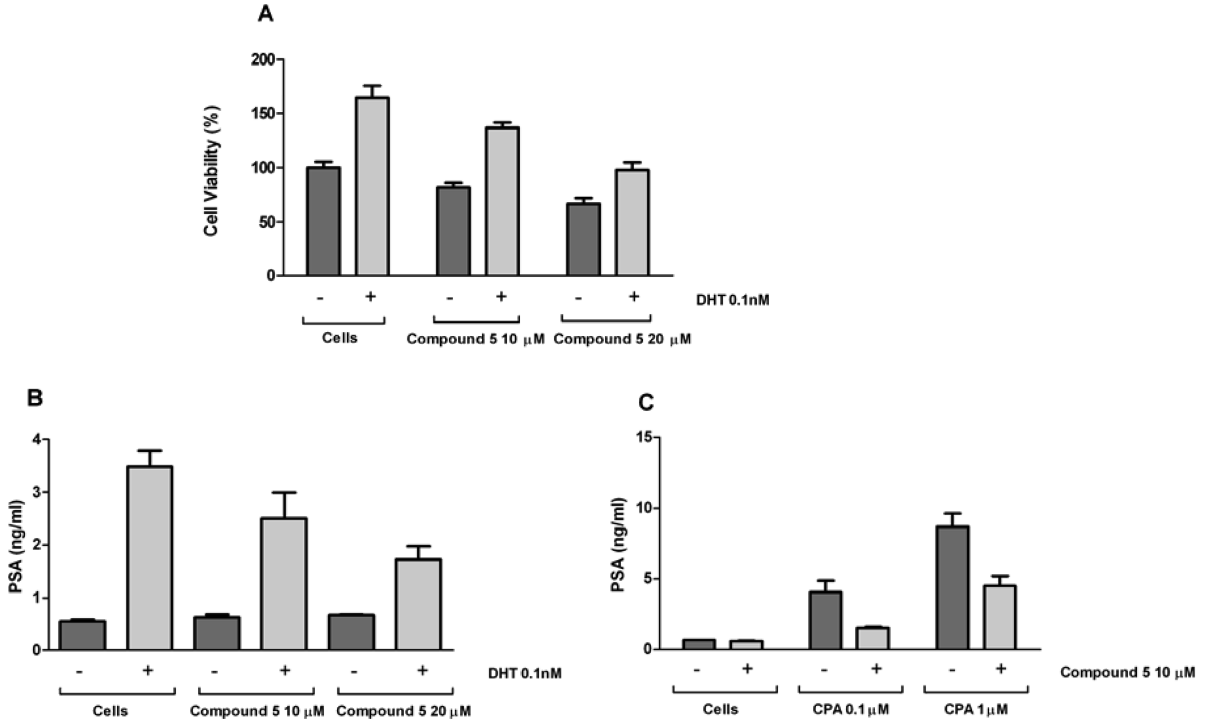

Figure 6. Effect of compound **5** on DHT- and CPA-stimulated cell proliferation. (A and B) **5** reduces androgen-stimulated cell growth and DHT-dependent AR signaling measured as PSA levels secreted in the cellular media in a dose-dependent fashion. (C) **5** at 10 μM reduces CPA-induced AR signaling (in absence of androgens) measured as PSA levels secreted in the cellular media in a dose-dependent fashion. Data are presented as the mean of two independent experiments, and bars show SEM for n = 6 values (A). Secreted PSA (ng/mL) was measured considering the optical density at 450 nm minus the optical density at 540 nm and interpolating the values from the standard curve. Data are presented as mean of two independent experiments, and bars show SEM for n = 4 values (B and C).

similar effects in this alternate system, supporting the hypothesis of their functioning as true antiandrogens (Supporting Information, Supplementary Figure 7).

DISCUSSION

Classical antiandrogen therapy is known to have limited beneficial effects in hormone-insensitive PCa. Alternative AR inhibitors are therefore needed in the treatment of PCa. In this study, we demonstrate the successful implementation of a virtual screening approach in the identification of small molecule AR modulators, where the structural motif of AR coactivators was included in a 3D pharmacophore. We report the discovery, identification, and characterization of a novel series of diarylhydrazide non-LBP-binding antiandrogen compounds, with demonstrated ability to displace AR coactivators and with established potency in AR-dependent prostate cancer cell lines. Activity was measured with a TR-FRET assay and a non-LBP-mediated mechanism of inhibition was confirmed by FP assay. These compounds are shown to function without any demonstrated intrinsic or partial agonist activity in AR and therefore can be classified as true[5] non-LBP antiandrogens.

The nature of NR coactivators and the high homology of NR coactivator binding sites are such that, to more fully profile the potential utility of these ligands, their selectivity was evaluated across members of the subclass of steroid receptors, including ER-α and ER-β, GR, AR, and PR.

The selectivity of the diarylhydrazide scaffold for the AR was demonstrated through TR-FRET evaluation in the estrogen and glucocorticoid receptors, where agonist bound receptor recruitment of coactivator was unimpaired at screening concentrations up to 100 μM.

We additionally investigated the potential cytotoxicity of the diarylhydrazides in three different cell lines, selecting **5** for its

dx.doi.org/10.1021/jm201438f | J. Med. Chem. 2012, 55, 1635–1644

favorable cytotoxic profile (cell viability was retained at around 80% in different prostatic cellular models).

Unmodified diarylhydrazide screening hits were also shown to have 2-fold selectivity for AR over PR, with partial antagonist activity demonstrated for the scaffolds in a PR functional assay, remarkable given the high (>60%) homology of these NR family members.[2,37] Futhermore, given the established utility of mifepristone (a PR modulator which also has antiandrogenic activity) in the treatment of castration resistant prostate cancer,[38,39] the narrower selectivity window observed for these AR ligands in PR over the other NR's assessed is not a significant concern in the context of the therapeutic area under consideration.

Classical antiandrogens can be also distinguished for their different behaviors at a cellular level. Save for two recent examples,[20,21] all LBP antiandrogens described to date have also intrinsic partial agonist activity,[34] demonstrated by induction of PSA in the absence of hormone stimulation in LNCaP cells. In this study, the novel non-LBP diarylhydrazide antiandrogen **5** did not induce PSA expression in absence of hormone stimulation when compared to CPA. In androgen-deprived LNCaP cells, **5** reduces PSA expression in combination with CPA, antagonizing its partial agonist activity in a dose responsive fashion. This result supports the hypothesis of a nonclassical mechanism of AR inhibition for these diarylhydrazide ligands and it also demonstrates the potential application of these and other non-LBP antiandrogen small molecules targeting alternative AR sites in combination with existing prostate cancer therapy.

■ CONCLUSION

Through application of virtual screening methodologies, we present and characterize novel diarylhydrazide scaffolds as true antiandrogens—displacing AR−coactivator interaction and having a full antagonistic profile on AR (both wt and T877A), partial antagonistic profile for PR, and selectivity for the other members of the NR-3 family (GR, ER-α, and ER-β).

The initial small molecule non-LBP true AR modulators provided by this study will be used to further characterize the AR−coactivator interface, to understand the basis of selectivity, and to further guide rational drug design in the search of other novel scaffolds directed at this interface. Chemical optimization of the hydrazide linker to afford more tractable "druglike" compounds is currently underway.

■ EXPERIMENTAL SECTION

Time-Resolved Fluorescence Resonance Energy Transfer (TR-FRET). Lanthascreen TR-FRET AR Coactivator Assay Kit (Invitrogen, cat no. PV4381) was used to screen for potential coactivator disruptors. Black, low volume, 384-well assay plates (Corning, NY, cat. no. 3676) were used to perform the assay (total volume 20 μL), and TR-FRET signal was measured with PHERAstar equipment (BMG LabTech) using a Lanthascreen optic module (excitation, 335 nm; emission, 520 nm channel A and 495 nm channel B).

TR-FRET values were calculated at 10 flashes per well, using a delay time of 100 μs and integration time 200 μs as recommended by the Invitrogen assay guidelines. The ratio 520 nm/495 nm was then calculated and plotted against the concentration. A serial dilution of compounds was first prepared in 100× DMSO (Sigma-Aldrich) starting from the maximum desired concentration to achieve a 12 point range concentration using 96-well polypropylene plates (Nalgene Nunc, Rochester, NY). Each 100× solution was diluted to 2× concentration with TR-FRET coregulator buffer A (Invitrogen proprietary buffer), yielding a final concentration of 1% DMSO in each well. Ten microliters of 2× solution was then added to the 384-well plate, following addition of 5 μL of 4× AR-LBD and 5 μL of D11-FxxLF/Tb anti-GST antibody in agonist mode and 5 μL of D11-FxxLF/Tb anti-GST antibody/DHT (included at a concentration equal to EC_{80} as determined by running the assay in agonist mode first).

$$EC_{80} = 10^{\{(\log EC_{50}) + [(1/\text{Hill slope}) \log[80/(100-80)]]\}}$$

D11-FxxLF and Tb antibody were premixed in light protecting vials prior to use. A final concentration of 5 mM DTT was used in the assay buffer in order to prevent protein degradation. All plates (agonist and antagonist mode) were incubated between 2 and 4 h at room temperature protected from light prior to TR-FRET measurement. IC_{50} values were determined by testing each ligand at concentrations ranging from 100 μM to 45 nM using 2- and 3-fold dilutions to generate a 12 point dose−response curve. Data was fitted using the sigmoidal dose response (variable slope) available from Graphpad Prism 5.[40]

$$Y = \text{Bottom} + (\text{Top} - \text{Bottom}) \Big/ \left(1 + 10^{[(\log IC_{50} - X)(\text{Hill slope})]}\right)$$

The Z factor for these assays was >0.5, as calculated by the equation provided by Zhang et al.[41]

$$Z = 1 - \frac{3x(\sigma_p + \sigma_n)}{|\mu_p - \mu_n|}$$

In line with the assay protocol, a known agonist, dihydrotestosterone (DHT, cat no. A8380, Sigma), and a known antagonist, cyproterone acetate (cat no. C3412, Sigma), were used as controls in the assay. A control with no AR-LBD present was included to account for diffusion-enhanced FRET or ligand-independent coactivator recruitment. A negative control with 2× DMSO was present to account for any solvent vehicle effects.

The same procedure was used for AR T877A (Invitrogen cat no. PV4667), PR (Invitrogen cat no. PV4666), ER-α (Invitrogen cat no. PV4544), ER-β (Invitrogen cat no. PV4541), and GR (Invitrogen cat no. PV4683). The assay was adapted to exclude possible nonspecific aggregation mechanism of inhibition by adding very low concentration of detergent Triton X-100 (0.01%) to the assay buffer following the Shoichet review guidelines[42] (Supporting Information, Supplementary Figure 1).

Fluorescence Polarization (FP). PolarScreen Androgen Receptor Competitor Assay Kit Green (Invitrogen, cat no. P3018) was used to investigate the binding of the test compound to the LBP site, occupied by a high-affinity fluorophore ligand (Fluormone).

The 100× test compound solutions in DMSO were diluted in AR green buffer (Invitrogen) to achieve 2× concentrations and placed in a 384-well plate (Corning, cat no. 3576) with 40 μL volume capacity. AR-LBD was supplemented with 5 mM DTT to prevent protein degradation. AR-LBD and Fluormone (2×) mix were prepared separately and then added to each compound dilution to achieve a final concentration LBD-Fluormone of 50 and 2 nM, respectively. Plates were incubated protected from light for at least 4 h. Controls included a maximum mP positive control, which consists of the AR-LBD and Fluormone mix (2×), and a minimum mP control, containing only Fluormone (2×). A vehicle control was added to account for DMSO effect, and a blank control containing buffer only. Fluorescence polarization was measured with PHERAstar equipment (BMG LabTech) using an optic module with excitation at 485 nm and emission at 530 nm.

Cell Culture. LNCaP cells (androgen-dependent), PC-3 (androgen-independent), and PWR-1E (normal prostatic epithelia) were cultured in RPMI-1640 GlutaMAX (Invitrogen), F12K (Invitrogen), and K-SFM media (Invitrogen). The first two were supplemented with 10% fetal bovine serum (FBS), penicillin (100 units/mL), and streptomycin (100 μg/mL). K-SFM was supplemented with 5 ng/mL

epidermal growth factor (EGF) and 0.05 mg/mL bovine pituitary extract (BPE). Cells were propagated at 1:3 or 1:6 dilutions at 37 °C in 5% CO_2.

Cell Viability and Cell Proliferation Assays. For cell viability (end point) assays LNCaP, PC-3, and PWR-1E cells were seeded at 2.5×10^4/mL density in 200 μL volume of a 96-well plate in triplicate and incubated for 24 h prior testing. Test compounds were included at different concentrations to achieve a final concentration of 0.5% DMSO in each well. The effect of 0.5% DMSO on cell viability was also evaluated. Cell viability was assessed after 24 h of treatment using 10% AlamarBlue reagent (Invitrogen) for each well. Cell viability was monitored by the reduction of resazurin, a blue, cell-permeable, nontoxic compound, to resorufin, a red and highly fluorescent product. Viable cells continuously convert resazurin to resorufin, increasing the overall color and fluorescence of the media surrounding cells. Fluorescence intensity can be quantitatively determined with a fluorescence microplate reader at excitation/emission 544 nm/590 nm (Spectramax Gemini).

For hormone-dependent cell proliferation assays in androgen-deprived LNCaP cells, cells were seeded at 2×10^4 cells/mL in a 24-well plate in triplicate. Cells were plated in phenol red free RPMI GlutaMAX (Invitrogen) supplemented with 10% charcoal-stripped FBS to deplete endogenous steroids 48 h prior to the assay, as described in previous reports.[43] The optimal condition for the treatment was found to be 5 days and the concentration of DHT included to stimulate the cells was 0.1 nM. Cells were treated with different concentrations of test compounds with or without 0.1 nM DHT to achieve a final concentration of 0.1% DMSO in each well. A control for the vehicle was included to ensure that no effect on viability could be detected. Media and treatments were replaced every second day, after washing the cells twice with 1× PBS. Supernatants were collected after 5 days for evaluation of secreted PSA levels, and cell proliferation was assessed for the same plate using AlamarBlue in order to exclude nonspecific effects due to toxicity issues.

Prostate Specific Antigen (PSA) ELISA. Secreted levels of prostate specific antigen were evaluated with a commercially available kit (Quantikine Human Kallikrein 3/PSA Immunoassay, R&D systems). The assay was performed following manufacturer's guidelines. In brief, 50 μL of standards and cell culture samples were added to precoated wells containing assay diluent RD1W (R&D systems) and incubated for 2 h at room temperature. Unbound material was washed several times and 200 μL of horseradish peroxidase (HRP) labeled PSA conjugate antibody was added to each well and further incubated for 2 h at room temperature. Wells were washed and treated with colored substrate (tetramethylbenzidine) for an additional 30 min, after which 50 μL of stop solution (2 N sulfuric acid) was added per well and optical density (450 nm with correction at 540 nm) was read with a plate reader within 30 min (Versamax).

Molecular Modeling. A virtual screen was designed to select compounds mapping onto the peptide binding surface (AF2) of the AR receptor, based on an ensemble of documented X-ray crystal structures (PDB ID 1T73, 1T74, 1T76, 1T79, 1T7F, 1T7M, 1T7R, and 1T7T).[23] Molecular Operating Environment (MOE) software[25] was employed to preprocess the proteins and to remove the coactivator peptides from the complexes. An initial pharmacophore was generated using the MOE pharmacophore elucidator and considering the most significant features, which involved hydrophobic, donor, and acceptor features. A second pharmacophore was developed including two additional hydrophobic/aromatic features to represent the Phe side chains present in the FxxLF coactivator motif (1T7R), so as to increase the selectivity for AR over other families of nuclear receptor. These pharmacophore models were then applied for in silico screens of small-molecule commercial libraries to identify compounds that resemble the "active principle" of the starting peptides.[44]

Database Preprocessing. A number of vendor databases were selected for screening of ligands, including Amsterdam[45] (5389 compounds), Peakdale[46] (8188), Asinex[47] Platinum collection (75 258), Specs[48] (175 800), Maybridge[49] (56 870), and ZINC[50,51] (4.6 million) compounds. A Bayesian analysis was performed on the peptide structures to estimate parameters of an underlying distribution based on the observed distribution. The above databases were then filtered for those compounds with properties similar to the peptides, thus focusing the search on the AR ligand chemical space. Any salts or duplicates were removed. All molecules were standardized for stereochemistry and charges and ionized at a pH of 7.4 and all calculable tautomers were enumerated. At this stage the conformational flexibility of the screening compounds was explored using the Omega software[52] (OpenEye Scientific package). A maximum of 50 conformations were generated for each molecule in the data set.

Compound Screening. The virtual molecules were overlaid on and compared to the generated pharmacophore of the active ligands, and those molecules that compared favorably were advanced for additional virtual screening and scoring. The Fast Rigid Exhaustive Docking (FRED)[53] software as implemented in OpenEye Scientific's package was used to exhaustively examine all possible poses within the protein site, filtering for shape complementarity and scoring. The smaller databases (Amsterdam[45] and Peakdale[46]) were screened on all 13 crystal structures and only ligands scoring well on more than one crystal structure were considered. The larger databases Specs,[48] Asinex,[47] Maybridge,[49] and ZINC[50,51] were screened on the 1T7R crystal structure.

Similarity Search. A structural similarity search was conducted on **1** and **2** using a Tanimoto coefficient of >70% on the Specs compound database.[48] Thirty-seven compounds were purchased and four small molecules were selected for optimization and characterization studies based on their improved on-target activity determined by TR-FRET.

Compound General Information. All screening compounds described in this work were purchased as commercial samples from Specs NV.[48] Compound purity in all instances was greater than 95% as determined by LCMS and NMR.

■ ASSOCIATED CONTENT

Ⓢ Supporting Information

Full experimental protocols for the identification of true AR binders (TR-FRET and FP); TR-FRET data for GR, ER-α, and ER-β (five point dose−response curves); FP data for PR at a single point concentration; cell toxicity and hormone/CPA dependent data on 22Rv1 cells; and a table of all compounds tested during the investigation on AR TR-FRET. This material is available free of charge via the Internet at http://pubs.acs.org.

■ AUTHOR INFORMATION

Corresponding Author

*E-mail: lloyddg@tcd.ie. Phone: +353(1)8963527.

Present Address

[‖]The Marie Curie Laboratory for Membrane Proteins, Department of Biology, National University of Ireland, Maynooth, County Kildare, Ireland.

Notes

The authors declare no competing financial interest.

■ ACKNOWLEDGMENTS

The authors thank the Irish Health Research Board (HRB) (HRB/2007/2), Enterprise Ireland (EI- CFTD/06/110), and Cancer Research Ireland (CRI) for research funding. The Trinity Biomedical Sciences Institute is supported by a capital infrastructure investment from Cycle 5 of the Irish Higher Education Authority's Programme for Research in Third Level Institutions (PRTLI). L.C. thanks Prof. Robert Fletterick and his group (Fletterick lab, UCSF) for helpful discussions. F.B. thanks the support of the European Commission (Marie-Curie grant, People FP7, Project Reference: 274988). 22Rv1 cells were generously provided by Alice Vajda, Laure Marignol, and Prof. Donal Hollywood in the Prostate Cancer Research group (Institute of Molecular Medicine, Dublin).

■ ABBREVIATIONS USED

AF-1, activation function-1; AF-2, activation function-2; AR, androgen receptor; BF-3, binding function-3; BPE, bovine pituitary extract; CPA, cyproterone acetate; DBD, DNA-binding domain; DHT, dihydrotestosterone; ELISA, enzyme-linked immunosorbent assay; ER-α, estrogen receptor α; ER-β, estrogen receptor β; FBS, fetal bovine serum; FP, fluorescence polarization; FRED, fast rigid exhaustive docking; F12K, Kaighn's modification of Ham's F-12 medium; GR, glucocorticoid receptor; HH, harmol hydrochloride; HRP, horseradish peroxidase; K-SFM, keratinocyte serum free medium; LBD, ligand binding domain; LBP, ligand binding pocket; LNCaP, androgen-dependent human prostate cancer cell line; mP, millipolarization units; MOE, molecular operating environment; NA, not active; NR, nuclear receptor; PC-3, androgen-independent human prostate cancer cell line; PCa, prostate cancer; PGC-1α, peroxisome proliferator-activated receptor γ coactivator 1-α; PR, progesterone receptor; PP, pyrvinium pamoate; PSA, prostate-specific antigen; PWR-1E, androgen-dependent human prostatic cell line; RPMI, Roswell Park Memorial Institute; SEM, standard error of the mean; SRC, steroid receptor coactivator; Tb, terbium; tes, testosterone; TR-FRET, time-resolved fluorescence resonance energy transfer; VS, virtual screening; wt, wild-type; x, unspecified amino acid; 22Rv1, partially androgen-independent human prostate cancer cell line

■ REFERENCES

(1) Ferlay, J.; Shin, H. R.; Bray, F.; Forman, D.; Mathers, C.; Parkin, D. M. Estimates of worldwide burden of cancer in 2008: GLOBOCAN 2008. *Int. J. Cancer* **2010**, *127*, 2893−2917.

(2) Evans, R. M. The steroid and thyroid hormone receptor superfamily. *Science* **1988**, *240*, 889−895.

(3) Bain, D. L.; Heneghan, A. F.; Connaghan-Jones, K. D.; Miura, M. T. Nuclear receptor structure: Implications for function. *Annu. Rev. Physiol.* **2007**, *69*, 201−220.

(4) Estebanez-Perpina, E.; Arnold, L. A.; Nguyen, P.; Rodrigues, E. D.; Mar, E.; Bateman, R.; Pallai, P.; Shokat, K. M.; Baxter, J. D.; Guy, R. K.; Webb, P.; Fletterick, R. J. A surface on the androgen receptor that allosterically regulates coactivator binding. *Proc. Natl. Acad. Sci. U. S. A.* **2007**, *104*, 16074−16079.

(5) Chen, Y.; Clegg, N. J.; Scher, H. I. Anti-androgens and androgen-depleting therapies in prostate cancer: New agents for an established target. *Lancet Oncol.* **2009**, *10*, 981−991.

(6) Gregory, C. W.; He, B.; Johnson, R. T.; Ford, O. H.; Mohler, J. L.; French, F. S.; Wilson, E. M. A mechanism for androgen receptor-mediated prostate cancer recurrence after androgen deprivation therapy. *Cancer Res.* **2001**, *61*, 4315−4319.

(7) Feldman, B. J.; Feldman, D. The development of androgen-independent prostate cancer. *Nat Rev Cancer* **2001**, *1*, 34−45.

(8) Gunther, J. R.; Parent, A. A.; Katzenellenbogen, J. A. Alternative inhibition of androgen receptor signaling: Peptidomimetic pyrimidines as direct androgen receptor/coactivator disruptors. *ACS Chem. Biol.* **2009**, *4*, 435−440.

(9) Axerio-Cilies, P.; Lack, N. A.; Nayana, M. R.; Chan, K. H.; Yeung, A.; Leblanc, E.; Guns, E. S.; Rennie, P. S.; Cherkasov, A. Inhibitors of androgen receptor activation function-2 (AF2) site identified through virtual screening. *J. Med. Chem.* **2011**, *54*, 6197−6205.

(10) Rodriguez, A. L.; Tamrazi, A.; Collins, M. L.; Katzenellenbogen, J. A. Design, synthesis, and in vitro biological evaluation of small molecule inhibitors of estrogen receptor alpha coactivator binding. *J. Med. Chem.* **2004**, *47*, 600−611.

(11) Acevedo, M. L.; Lee, K. C.; Stender, J. D.; Katzenellenbogen, B. S.; Kraus, W. L. Selective recognition of distinct classes of coactivators by a ligand-inducible activation domain. *Mol. Cell* **2004**, *13*, 725−738.

(12) LaFrate, A. L.; Gunther, J. R.; Carlson, K. E.; Katzenellenbogen, J. A. Synthesis and biological evaluation of guanylhydrazone coactivator binding inhibitors for the estrogen receptor. *Bioorg. Med. Chem.* **2008**, *16*, 10075−10084.

(13) Hwang, J. Y.; Huang, W.; Arnold, L. A.; Huang, R.; Attia, R. R.; Connelly, M.; Wichterman, J.; Zhu, F.; Augustinaite, I.; Austin, C. P.; Inglese, J.; Johnson, R. L.; Guy, R. K. Methylsulfonylnitrobenzoates, a new class of irreversible inhibitors of the interaction of the thyroid hormone receptor and its obligate coactivators that functionally antagonizes thyroid hormone. *J. Biol. Chem.* **2011**, *286*, 11895−11908.

(14) York, B.; O'Malley, B. W. Steroid receptor coactivator (SRC) family: Masters of systems biology. *J. Biol. Chem.* **2010**, *285*, 38743−38750.

(15) Fletterick, R. J. Molecular modelling of the androgen receptor axis: Rational basis for androgen receptor intervention in androgen-independent prostate cancer. *BJU Int.* **2005**, *96* (Suppl 2), 2−9.

(16) Chang, C. Y.; McDonnell, D. P. Androgen receptor-cofactor interactions as targets for new drug discovery. *Trends Pharmacol. Sci.* **2005**, *26*, 225−228.

(17) Joseph, J. D.; Wittmann, B. M.; Dwyer, M. A.; Cui, H.; Dye, D. A.; McDonnell, D. P.; Norris, J. D. Inhibition of prostate cancer cell growth by second-site androgen receptor antagonists. *Proc. Natl. Acad. Sci. U. S. A.* **2009**, *106*, 12178−12183.

(18) Moore, T. W.; Mayne, C. G.; Katzenellenbogen, J. A. Minireview: Not picking pockets: Nuclear receptor alternate-site modulators (NRAMs). *Mol. Endocrinol.* **2010**, *24*, 683−695.

(19) Fletterick, R. J.; Estebanez-Perpina, E.; Jouravel, N. Perspectives on designs of antiandrogens for prostate cancer. *Expert Opin. Drug Discovery* **2007**, *2*, 1341−1355.

(20) Scher, H. I.; Beer, T. M.; Higano, C. S.; Anand, A.; Taplin, M. E.; Efstathiou, E.; Rathkopf, D.; Shelkey, J.; Yu, E. Y.; Alumkal, J.; Hung, D.; Hirmand, M.; Seely, L.; Morris, M. J.; Danila, D. C.; Humm, J.; Larson, S.; Fleisher, M.; Sawyers, C. L. Antitumour activity of MDV3100 in castration-resistant prostate cancer: A phase 1−2 study. *Lancet* **2010**, *375*, 1437−1446.

(21) Tran, C.; Ouk, S.; Clegg, N. J.; Chen, Y.; Watson, P. A.; Arora, V.; Wongvipat, J.; Smith-Jones, P. M.; Yoo, D.; Kwon, A.; Wasielewska, T.; Welsbie, D.; Chen, C. D.; Higano, C. S.; Beer, T. M.; Hung, D. T.; Scher, H. I.; Jung, M. E.; Sawyers, C. L. Development of a second-generation antiandrogen for treatment of advanced prostate cancer. *Science* **2009**, *324*, 787−790.

(22) Jones, J. O.; Bolton, E. C.; Huang, Y.; Feau, C.; Guy, R. K.; Yamamoto, K. R.; Hann, B.; Diamond, M. I. Non-competitive androgen receptor inhibition in vitro and in vivo. *Proc. Natl. Acad. Sci. U. S. A.* **2009**, *106*, 7233−7238.

(23) Hur, E.; Pfaff, S. J.; Payne, E. S.; Gron, H.; Buehrer, B. M.; Fletterick, R. J. Recognition and accommodation at the androgen receptor coactivator binding interface. *PLoS Biol* **2004**, *2*, E274.

(24) He, B.; Minges, J. T.; Lee, L. W.; Wilson, E. M. The FXXLF motif mediates androgen receptor-specific interactions with coregulators. *J. Biol. Chem.* **2002**, *277*, 10226−10235.

(25) *MOE. 2010.10*; Chemical Computing Group: Montreal, 2010; www.chemcomp.com.

(26) *PyMOL*; PyMOL DeLano Scientific LLC.

(27) Gunther, J. R.; Du, Y.; Rhoden, E.; Lewis, I.; Revennaugh, B.; Moore, T. W.; Kim, S. H.; Dingledine, R.; Fu, H.; Katzenellenbogen, J. A. A set of time-resolved fluorescence resonance energy transfer assays for the discovery of inhibitors of estrogen receptor-coactivator binding. *J. Biomol. Screen.* **2009**, *14*, 181−193.

(28) Gaddipati, J. P.; McLeod, D. G.; Heidenberg, H. B.; Sesterhenn, I. A.; Finger, M. J.; Moul, J. W.; Srivastava, S. Frequent detection of codon 877 mutation in the androgen receptor gene in advanced prostate cancers. *Cancer Res.* **1994**, *54*, 2861−2864.

(29) Veldscholte, J.; Berrevoets, C. A.; Ris-Stalpers, C.; Kuiper, G. G.; Jenster, G.; Trapman, J.; Brinkmann, A. O.; Mulder, E. The androgen receptor in LNCaP cells contains a mutation in the ligand binding domain which affects steroid binding characteristics and response to antiandrogens. *J Steroid Biochem. Mol. Biol.* **1992**, *41*, 665−669.

(30) Horoszewicz, J. S.; Leong, S. S.; Chu, T. M.; Wajsman, Z. L.; Friedman, M.; Papsidero, L.; Kim, U.; Chai, L. S.; Kakati, S.; Arya, S. K.; Sandberg, A. A. The LNCaP cell line—A new model for studies on human prostatic carcinoma. *Prog Clin Biol Res* **1980**, *37*, 115−132.
(31) Kaighn, M. E.; Narayan, K. S.; Ohnuki, Y.; Lechner, J. F.; Jones, L. W. Establishment and characterization of a human prostatic carcinoma cell line (PC-3). *Invest. Urol.* **1979**, *17*, 16−23.
(32) Webber, M. M.; Bello, D.; Kleinman, H. K.; Wartinger, D. D.; Williams, D. E.; Rhim, J. S. Prostate specific antigen and androgen receptor induction and characterization of an immortalized adult human prostatic epithelial cell line. *Carcinogenesis* **1996**, *17*, 1641−1646.
(33) Balk, S. P.; Ko, Y. J.; Bubley, G. J. Biology of prostate-specific antigen. *J. Clin. Oncol.* **2003**, *21*, 383−391.
(34) Chen, C. D.; Welsbie, D. S.; Tran, C.; Baek, S. H.; Chen, R.; Vessella, R.; Rosenfeld, M. G.; Sawyers, C. L. Molecular determinants of resistance to antiandrogen therapy. *Nat. Med.* **2004**, *10*, 33−39.
(35) Wong, C.; Kelce, W. R.; Sar, M.; Wilson, E. M. Androgen receptor antagonist versus agonist activities of the fungicide vinclozolin relative to hydroxyflutamide. *J. Biol. Chem.* **1995**, *270*, 19998−20003.
(36) Sramkoski, R. M.; Pretlow, T. G. 2nd; Giaconia, J. M.; Pretlow, T. P.; Schwartz, S.; Sy, M. S.; Marengo, S. R.; Rhim, J. S.; Zhang, D.; Jacobberger, J. W. A new human prostate carcinoma cell line, 22Rv1. *In Vitro Cell Dev. Biol. Anim.* **1999**, *35*, 403−409.
(37) Mangelsdorf, D. J.; Thummel, C.; Beato, M.; Herrlich, P.; Schutz, G.; Umesono, K.; Blumberg, B.; Kastner, P.; Mark, M.; Chambon, P.; Evans, R. M. The nuclear receptor superfamily: The second decade. *Cell* **1995**, *83*, 835−839.
(38) Song, L. N.; Coghlan, M.; Gelmann, E. P. Antiandrogen effects of mifepristone on coactivator and corepressor interactions with the androgen receptor. *Mol. Endocrinol.* **2004**, *18*, 70−85.
(39) Taplin, M. E.; Manola, J.; Oh, W. K.; Kantoff, P. W.; Bubley, G. J.; Smith, M.; Barb, D.; Mantzoros, C.; Gelmann, E. P.; Balk, S. P. A phase II study of mifepristone (RU-486) in castration-resistant prostate cancer, with a correlative assessment of androgen-related hormones. *BJU Int.* **2008**, *101*, 1084−1089.
(40) *Prism. 5.01*; GraphPad Software: San Diego, CA; www.graphpad.com
(41) Zhang, J. H.; Chung, T. D.; Oldenburg, K. R. A simple statistical parameter for use in evaluation and validation of high throughput screening assays. *J. Biomol. Screen.* **1999**, *4*, 67−73.
(42) Shoichet, B. K. Screening in a spirit haunted world. *Drug Discovery Today* **2006**, *11*, 607−615.
(43) Liu, S.; Yuan, Y.; Okumura, Y.; Shinkai, N.; Yamauchi, H. Camptothecin disrupts androgen receptor signaling and suppresses prostate cancer cell growth. *Biochem. Biophys. Res. Commun.* **2010**, *394*, 297−302.
(44) Hummel, G.; Reineke, U.; Reimer, U. Translating peptides into small molecules. *Mol. Biosyst.* **2006**, *2*, 499−508.
(45) Amsterdam: In Vrije Universiteit, Faculteit der Exacte Wetenschappen, afdeling Farmacochemie.
(46) Peakdale: www.peakdale.co.uk.
(47) Asinex: www.asinex.com.
(48) Specs: www.specs.net.
(49) Maybridge: www.maybridge.com
(50) ZINC: http://zinc.docking.org
(51) Irwin, J. J.; Shoichet, B. K. ZINC—A free database of commercially available compounds for virtual screening. *J. Chem. Inf. Model.* **2005**, *45*, 177−182.
(52) *OMEGA*; OpenEye Scientific Software: Santa Fe, NM; www.eyesopen.com.
(53) *FRED. 2.2.3*; OpenEye Scientific Software: Santa Fe, NM; www.eyesopen.com.